 DOI: 10.1002/masy.200950531

Poly(methyl methacrylate) Membrane: Dynamic Measurement of Concentrations During Water-Induced Phase Separation

Mohammad Karimi, Mohammad Haghighat Kish*

Summary: The properties of membranes produced by nonsolvent-induced phase separation (NIPS) depend on the rate of mass transfer of mobile components. This paper reports the use of Fourier transform infrared-attenuated total reflectance (FTIR-ATR) using principle component regression (PCR) analysis to study the compositional change of polymer solution immersed into the water prior to the phase demixing. To correlate the compositional change with the macroscopic structure, the observation on the dynamics of NIPS is made by a low magnification optical microscope equipped with a video camera. The morphology of the films was also examined by scanning electron microscope. Acetone and N, N-dimethylformamide were chosen as solvents to present different behavior of poly (methyl methacrylate) (PMMA) solutions during the NIPS process. The ratio of solvent and nonsolvent exchange, flux ratio $d\phi_2/d\phi_1$ shows the mass transfer in the homogeneous polymer solution after immersion in a nonsolvent bath. The results show that the flux ratio ($d\phi_2/d\phi_1$) is affected by solvents which probably affects the ultimate structures of the precipitated polymer.

Keywords: flux ratio; FTIR-ATR; membrane; nonsolvent-induced phase separation; structure

Introduction

Porous polymeric materials in the shapes of hollow fiber or membranes have a broad industrial application for separation of gases and filtration of liquids. The use of a polymeric membrane depends on their morphology that is developed during the formation process. There are several methods for polymer membrane preparation. Frequently nonsolvent- induced phase separation (NIPS) is applied.[1–2] During the NIPS process a polymer solution consisting of a polymer and a solvent or sometimes a mixture of solvent with a small amount of additive is casted and then immersed in a large-volume bath of nonsolvent. The nonsolvent has to be miscible with the solvent. The exchange of the solvent and the nonsolvent across the interface initiates the phase separation of the polymer solution in two phases; one with a high polymer concentration (polymer-rich phase), and the other with a low polymer concentration (polymer-lean phase). The concentrated phase solidifies soon after the phase separation. The diluted phase forms the pores. These two phases generate a specific texture of the precipitate (macroscopic structure). The ultimate morphology in macroscopic and microscopic scale varies depending on the properties of the materials and the process conditions. The morphology of the membranes, the most favorable feature, is strongly related to the composition of the casting film prior and during the immersion precipitation. The compositional change during the phase separation has been frequently discussed theoretically,[3–5] but the experimental results for the composition of the homogeneous polymer solution prior to precipitation of polymer are scarce.[6,7]

Amirkabir University of Technology, Department of Textile Engineering, Hafez Avenue, Iran-15914 Tehran, Iran
Fax: +98-21-66400245;
E-mail: mkarimi@aut.ac.ir

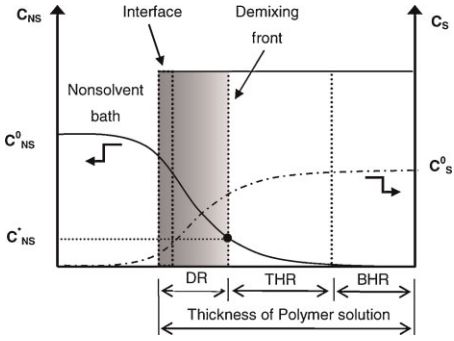

Figure 1.
Schematic representation of the concentration profiles of nonsolvent C_{NS} and solvent C_S during NIPS. C^0_{NS} and C^0_S are the initial concentration of nonsolvent and solvent in coagulation bath and polymer solution, respectively. C^*_{NS} is the critical nonsolvent concentration in polymer solution.

Figure 1 shows a schematic representation of the concentration profiles of the solvent and nonsolvent for a typical NIPS induced demixing process in a cast film.

There are three regions in the cast polymer solution; demixed region (DR), ternary homogenous region (THR) and binary homogenous region (BHR) that are shown on the x axis. The main difference between THR and BHR is in the presence of nonsolvent. The amount of nonsolvent in the THR region is more than that in the BHR region. However both regions are homogenous solutions. The quantification of the components in the THR region, on the right hand side of demixing front, is required to understand the demixing process. In particular composition changes of all components prior to the demixing stage are necessary. Generally such information can not be acquired using microscope or transmission techniques because the polymer solution appears transparent in the homogeneous state. In order to find out the change of composition during the phase inversion process it needs to determine the rate of solvent outflow (J_1) and nonsolvent inflow (J_2) through the diffusion layer. By this measurement the calculation of the changes in polymer content becomes possible.

Different techniques have been used to characterize the NIPS process. Microscopy techniques were the first technique used to evaluate the location of the coagulation front.[8–11] Light transmissions during the contact of polymer solution and coagulation bath were also measured.[12–14] Both techniques are suitable to recognize the differences between an instantaneous and a delayed phase demixing process qualitatively or semi-quantitatively. These measurements lead to overall information characterizing the whole process of the phase inversion after separation of the phases. The dimensions of these phases were in order of micrometers.

Recently FTIR spectroscopy[7] as well as Raman spectroscopy[15,16] has been adapted to characterize the nonsolvent penetration into the diffusion layer. A spot near the interface of a thin layer of casting solution has been examined. There are two problems with these methods. One is the difficulty of introducing the nonsolvent (especially water) into the liquid cell by a syringe due to the capillary action of water. The other is the saturation of coagulation bath with solvent due to limitation of circulation in the nonsolvent bath. It seems that the investigations of the phase demixing processes by such arrangements limits the information about the compositional change prior the phase demixing step.

In the present work FTIR-ATR is used in a special arrangement to determine the concentration of components in the diffusion layers under quench condition prior to the phase separation and the concentration of all components in front of the coagulation boundary. This technique allows a simultaneous determination of solvent outflow and water inflow during the immersion time. Determination of the composition of all components becomes possible by using the calibration curves.

The structure formation of PMMA in different solvents is well-described in the literature[7,16–19] and it is chosen as a model system to verify the applicability of the proposed experimental technique. On the basis of the measurements the composition pathway in the homogeneous region of the ternary phase diagram is calculated.

Experimental Part

Materials

Poly (methyl methacrylate) (PMMA) was synthesized with the number average molecular weight Mn = 75000 g/mol and weight average molecular weight Mw = 84000 g/mol. Molecular weights were measured by Gel Permeation Chromatography (GPCV 2000-Waters, USA) using a calibration curve of polystyrene standards. Before solution preparation the polymer PMMA was dried at 110 °C in an oven for 4h. The polymer solutions (15.15 v/v %) were prepared by dissolution of the polymer at room temperature until a clear polymer solution was obtained. The solvents N, N-dimethylformamide (DMF) and acetone (AC) were obtained from Merck, Germany and used as received. Distilled water (H_2O) was used as nonsolvent. Characteristics of the polymer, solvents and nonsolvent used for the calculations are listed in Table 1.

FTIR-ATR Technique

Figure 2 shows the arrangement of ATR accessories. The polymer solution was cast directly on the surface of the flat crystal (ZnSe, a 45o ATR prism) equipped with a bottomless liquid cell. The depth of polymer solution that was equals to the film thickness was controlled by a Multi-Applicator (Gardner, Japan). The water was transferred into the cell and the recording of the spectrum was started simultaneously. FTIR-ATR spectrums were recorded by a Nexus 670 spectrometer in real time mode, allowing a measurement of a spectrum in 0.2 second. The spectrum was measured at a wave number resolution of 4 cm^{-1} as single scan for a spectral range from 4000 to 750 cm^{-1}. All the measurements were made at room temperature.

According to the principle of ATR technique,[20,21] the depth of penetration of IR beams is limited. The penetration depth of the IR beam in polymer solution sample can be calculated by Equation (1).

$$dp = \frac{\lambda}{2\pi(n_1^2 \sin^2\theta - n_2^2)^{1/2}} \quad (1)$$

where depth of penetration of evanescent wave is shown by dp, λ is the wavelength of the infrared radiation, n_1 and n_2 are the refractive indices of flat crystals and polymer solutions respectively and θ is the angle of incidence beam.[20,21]

The refractive index of polymer solution (n_2) was measured with a refractometer, ERMA Optical Works, Japan. The measured refractive index of PMMA/AC and PMMA/DMF are 1.384 and 1.436 respectively. Using IR radiation with the wave number ranging from 850 cm^{-1} to 3800 cm^{-1}, the value of $\theta = 45$, $n_1 = 2.4$ the value of dp is calculated. For PMMA/AC solution it changes between 1.91 μm and 0.41 μm while for PMMA/DMF solution it changes between 2.07 μm and 0.46 μm. With the addition of water in to the polymer solution, the refractive indexes of the mixtures are reduced. Calculations showed that dp is not considerably changed with the changes in the refractive indexes of polymer solution. The values of dp vary between 1.79 μm and 0.39 μm when the water is in contact with the crystal.

For determination of the concentration of all components by FTIR, the software TQ ANALYST,[22] using the principle component regression (PCR)[23] was used. The calibration of the system was accomplished by capturing spectrum from all pure components, binary and ternary mixtures with water, solvents and polymer. By means of the PCR technique it was possible to

Table 1.
Characteristics of the materials.

Materials	Specific volume (cm^3/mol)	Molecular weight (g/mol)	Density (g/cm^3)
PMMA	63 025	75 000	1.12
AC	73.33	58.08	0.792
DMF	77.34	73.09	0.945
water	18.07	18.02	0.997

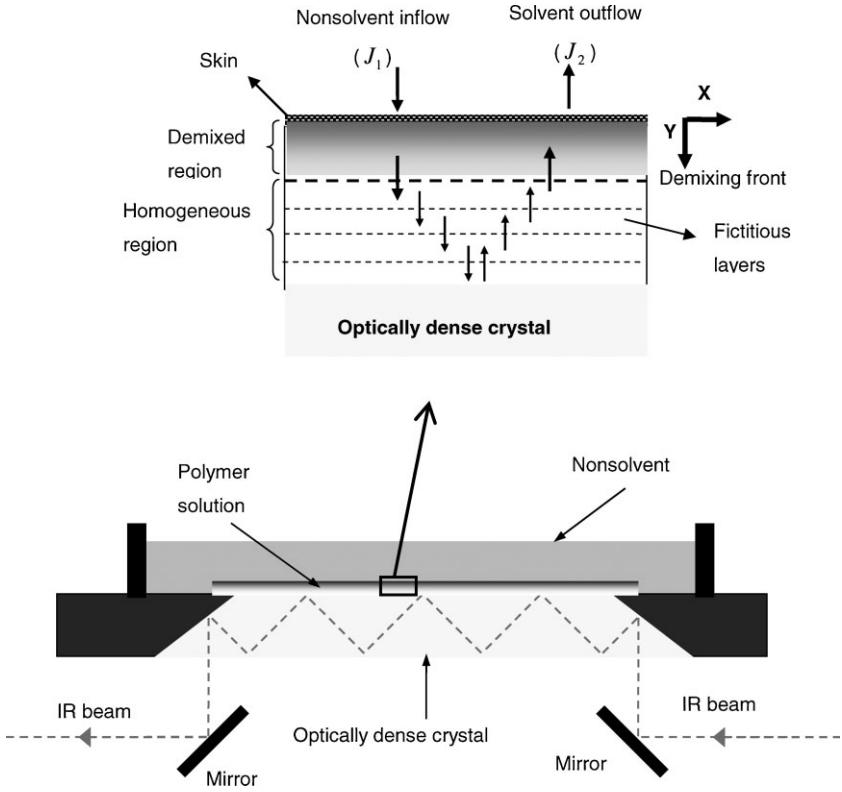

Figure 2.
Schematic representation of the ATR equipment (bottom) and project view of processes (top).

decouple and calibrate the component peaks or regions that overlap.

Optical Microscope Technique and Morphology Analysis

A drop of polymer solution was placed between two glass microscope slides and the nonsolvent (water) was injected with an analytical syringe. The exchange of solvent and nonsolvent was observed with the microscope (Carl Zeiss, Germany) equipped with a video camera for dynamic observation of the coagulation front. A videotape records the movement of the coagulation front at different time intervals. The speed of recording was 26 frames per second. The temperatures of the bath and solution during the experiments were room temperature. During the demixing of cast solution, the demixed area appears darker than the homogenous regions. All microphotographs chosen from videotape were analyzed by Adobe Photoshop software. The area of the demixed region was determined by means of a histogram of the darkness of images. The histogram illustrates how many pixels in an image are distributed by graphing the number of pixels at each color intensity level.[24]

SEM micrographs of different films were taken using a Cambridge S-360 scanning electron microscope. Films were fractured in liquid nitrogen and left at room temperature for a few days before testing. Samples for SEM microscopy were sputter-coated with gold before investigation.

Phase Diagrams

Cloud point was determined by titration method at 25 °C. A flask with a rubber septum stopper was charged with certain amount of polymer solutions and the weight of polymer

solution was measured. During the stirring by a mechanical stirrer the nonsolvents were introduced into the flask by a syringe through the septum. When turbidity of the solution was observed, composition at the cloud point was calculated using the measured volume of added water.

Results and Discussion

Observation of the Process by Microscope Technique

In Figures 3 and 4 the morphologies of both ternary systems are shown. These micrographs show the finger-like structure for H_2O/DMF/PMMA and sponge-like structures for H_2O/AC/PMMA systems.

Figure 3 represents a series of photomicrographs chosen from the videotape that documents the steps of the coagulation process of the H_2O/AC/PMMA system. In Figure 3-1 the smooth boundary shows the interface between the polymer solution and the nonsolvent (water). Upon introducing the water a planar demixing front is formed which moves inward, Figure 3-2 to 3-5. The demixed region (dark area) is the solid porous polymer phase; it is expanded to cover the dope by moving the demixing front inward (in the Y-direction as shown in the Figure 2). Finally after solidification, the so called sponge-like structure is remained, Figure 3–6. On the basis of the recorded photomicrographs, the time of the movement of the demixing front was determined by image processing technique. The demixing front moves at a rate that is proportional to the square root of time, which is studied by McHugh and co-workers.[25–28] This finding is in accordance to the Fickian diffusion that is often observed when the polymer chains have a high mobility.[29]

Figure 4 shows a series of selected videotape photomicrographs that indicates the steps of the coagulation process of the H_2O/DMF/PMMA system at different time. The smooth line represents the interface between the polymer solution and the nonsolvent bath (Figure 4-1). By introducing the water to the surrounding of the polymer solution, a group of finger pores was formed, which moves inward from the nonsolvent bath-dope interface. After a short period of time, a planar demixing front migrates inward and follows the fingers: Figures 4-2 to 4-5.

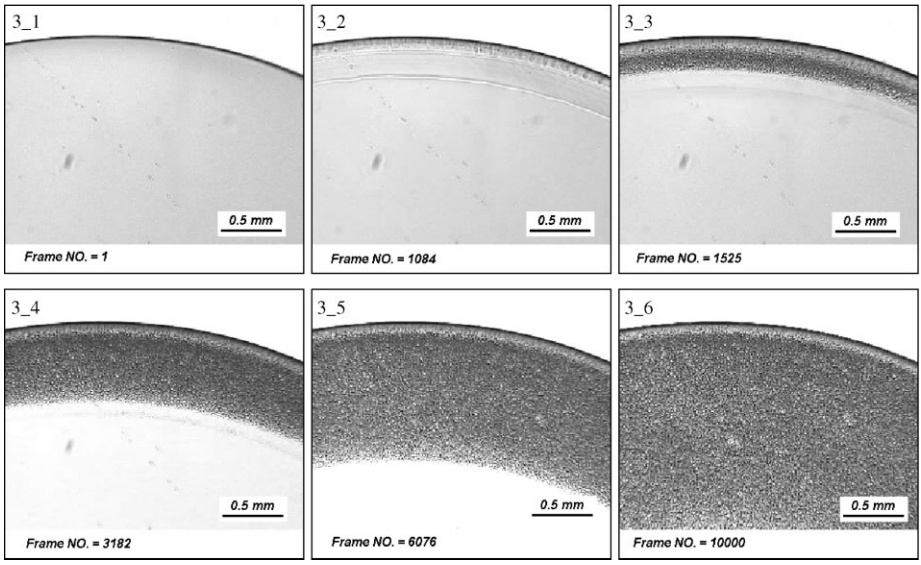

Figure 3.
Micrographs of the nonsolvent induced phase demixing process of the H_2O/AC/PMMA system using optical microscope technique.

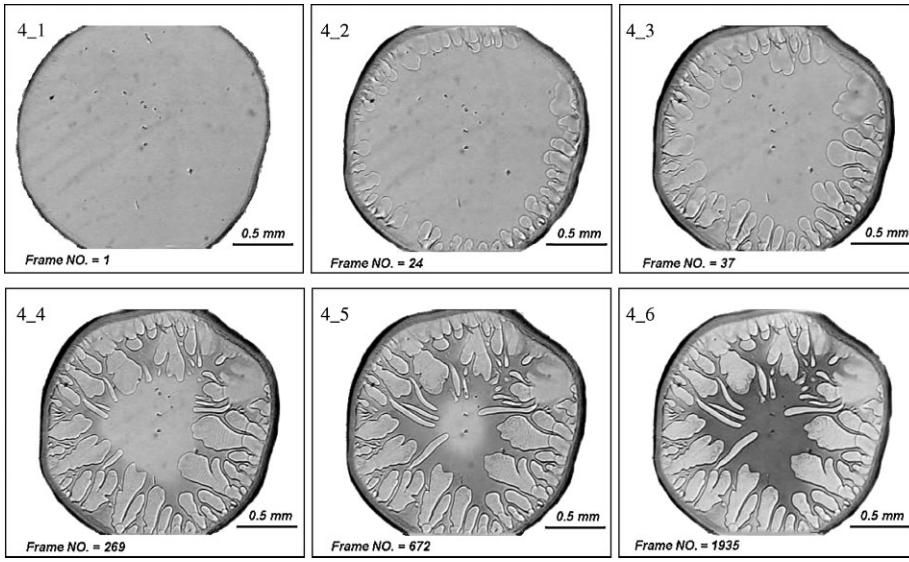

Figure 4.
Micrographs of the nonsolvent induced phase demixing process of the H_2O/DMF/PMMA system using optical microscope technique.

The moving fingers become surrounded by the demixing front and finally subsided after a longer period of time.

Figure 5 shows the demixing front distance from the skin vs. square root of time for both investigated systems. These results are consistent with the measured diffusion and gelation dynamics for cast films. During the time of gradual penetration of the water into the polymer/solvent system, the demixing front moves at two different slopes (Figure 5): in the initial period of the onset of precipitation, the movement of the demixing front is slow (in H_2O/AC/PMMA system). The sharp change of the slope in the movement of the demixing front is observed after about 35 seconds. In contrast the motion of the demixing front in the H_2O/DMF/PMMA system is found to start with a high initial slope corresponding to a rapid transfer of water into the solution. The rate is reduced because the boundary conditions are not completely fulfilled (too slow transfer of solvent in the nonsolvent bulk).

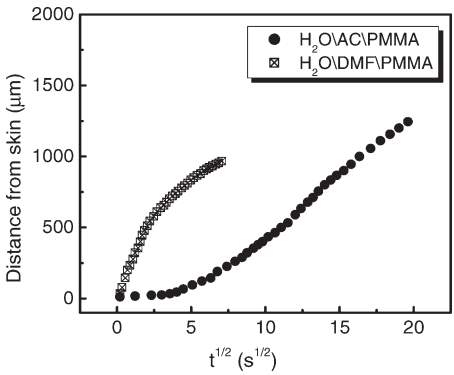

Figure 5.
Demixing front movement in H_2O/AC/PMMA and H_2O/DMF/PMMA systems in dependence on the square root of time.

It has been found that the rate of the movement of the demixing front follows the Fick's second law. In H_2O/DMF/PMMA system phase separation that immediately initiated followed the Fick's second law as long as the boundary condition of the model is completely fulfilled. This was realized only for the first stage of phase separation. In contrast, in H_2O/AC/PMMA system an induction period is related to a very lower rate of movement of the coagulation front. After the induction period, phase demixing starts, which also follows the Fick's second law.

Measurement of Changes in Composition during NIPS by FTIR-ATR Technique

Characterization of FTIR peaks

The absorbance spectra of pure H_2O, AC, DMF, and PMMA are presented in Figure 6. The region I (between 3800 cm^{-1} and 2750 cm^{-1}) verified the characteristic peak of water;[30] the intensity of this band is increased during the water penetration. The region II (between 1800 and 1525 cm^{-1}) includes characteristic peaks of AC, PMMA, DMF, and also water[30] that some of them overlap together in the mixture. The peak related to the presence of PMMA in the sample has an additional characteristic band between 1320 and 1050 cm^{-1}.[30] This range is introduced as region III in Figure 6.

Peak Decoupling and Quantifying of the Components

Figure 7 shows a series of spectra for both the H_2O/AC/PMMA and H_2O/DMF/PMMA systems. As can be seen in Figure 7-a (H_2O/AC/PMMA system), the characteristic peak of AC, 1710 cm^{-1}, severely overlaps with the PMMA peak at 1727 cm^{-1} but there is no overlapping with the characteristic peak of H_2O. As shown in Figure 7-b the characteristic peak of DMF overlaps with that of H_2O (1645 cm^{-1} and 1630 cm^{-1}) while the characteristic peak of PMMA does not overlap with the others. A decoupled program is used to estimate the area related to the contribution of different peaks. However it was not possible to obtain reproducible values for the area of the PMMA peak in H_2O/AC/PMMA system with low concentration of PMMA after the decoupling in this region. Thus the characteristic peak in the range of 1110–1200 cm^{-1} was used to quantify the PMMA concentration.[30]

The principle component regression (PCR) is used to resolve the bands in overlapped regions. This method was found to be satisfactory for solving complex analytical problems where the component peaks overlap.

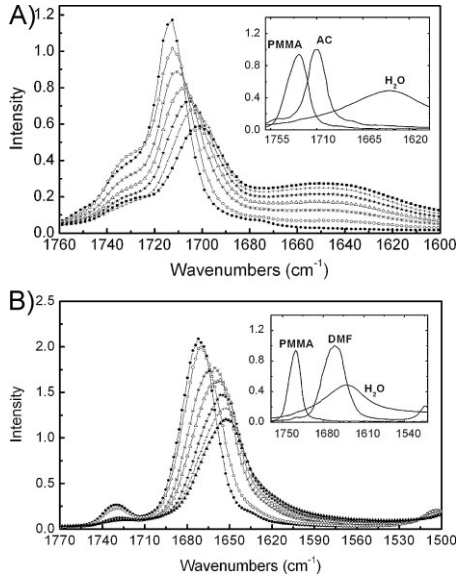

Figure 7.
Results of decoupling procedure for overlapped bands in evaluation region II. (A) H_2O/AC/PMMA system; (B) H_2O/DMF/PMMA system.

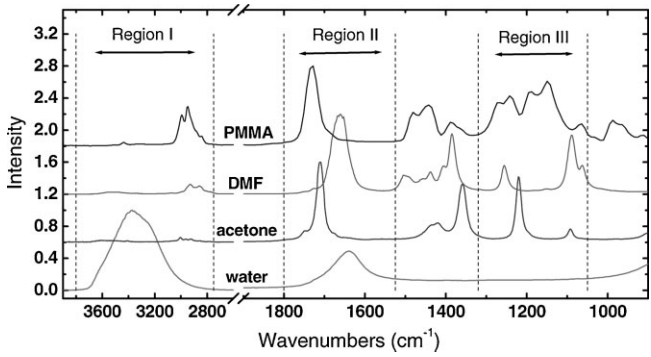

Figure 6.
ATR-IR spectra of PMMA, DMF, AC and water. The three regions marked have been used for calibration.

Calibration of the system was accomplished by capturing spectrum from all pure components and mixture of H_2O/solvent, solvent/PMMA and H_2O/solvent/PMMA.

Changes in Composition during the Immersion Precipitation Process

Having the FTIR-ATR spectrum measured and the system calibrated, the film composition was determined according to the method described in experimental part. Figures 8 and 9 show the change of concentration of polymer (ϕ_3) vs. the volume fraction of H_2O (ϕ_1) in H_2O/AC/PMMA and H_2O/DMF/PMMA systems in depth of 90, 140, and 240 micrometers from the interface during the NIPS process. The volume fraction of solvent decreased and the volume fraction of water increased with the time before polymer solution moves to and enter the heterogeneous region. This is related to the rate of solvent release and the water penetration. The changes of volume fraction of polymer in these systems differ in the trends as can be seen in the Figures. From the measured data the actual volume fraction of polymer was calculated from the flux ratio $d\phi_2/d\phi_1$ of solvent and nonsolvent according to Equation (2)

$$\phi_3 = \phi_{3,0} + \frac{d\phi_2}{d\phi_1}\phi_1 \qquad (2)$$

where ϕ_2 is the volume fraction of solvent, ϕ_1 is the volume fraction of nonsolvent, $\phi_{3,0}$ is the initial volume fraction of polymer, $\phi_1 + \phi_2 + \phi_3 = 1$, $d\phi_2/d\phi_1$ specifies the slope of the curve of ϕ_2 vs. ϕ_1. Dashed line is drawn parallel to the horizontal axis representing the case where the rate of solvent outflow (J_1) and the rate of water inflow (J_1) are identical (constant polymer concentration during the NIPS process).

For the H_2O/AC/PMMA system, in Figure 8, the rate of solvent outflow is higher than the water inflow in the all three layers. The volume fraction of polymer increases during the process. However the flux ratio $d\phi_2/d\phi_1$ for different layers was not identical. In the first period of time the solvent release is high near the interface with the ATR crystal (90 μm) and the trend of volume fraction of polymer vs. volume fraction of water has a steep inclination, as shown in the Figure 8. The region III (Figure 6) is chosen to analyze the characteristic peak of PMMA directly. Figure 10

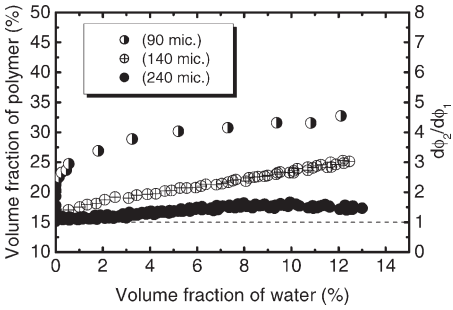

Figure 8.
Volume fraction of polymer vs. volume fraction of water during the NIPS process in dependence on the cast polymer solution thickness (H_2O/AC/PMMA system).

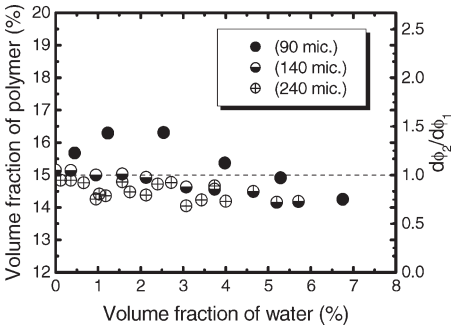

Figure 9.
Volume fraction of polymer vs. volume fraction of water during the NIPS process in dependence on the cast polymer solution thickness (H_2O/DMF/PMMA system).

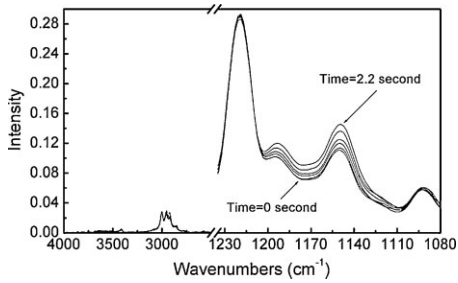

Figure 10.
IR spectra of compositional changes of polymer and water in the first 2.2 s of water contact (H_2O/AC/PMMA system).

shows a series of spectra for the H_2O/AC/PMMA system at a depth of 90 μm from the interface. During the first 2.2 seconds the characteristic peak of PMMA raises, that shows the increases in polymer content, but the characteristic peak of water (between 3800 cm^{-1} and 2750 cm^{-1}) remains practically unchanged. This result leads to the conclusion that the release of solvent without penetrating water is initiated by shrinkage in the upper layers of polymer solution. As obtained from the measurements the increase in polymer content in the upper layers of polymer solution increases when the delaying time in the phase demixing is increased. This finding is in agreement with the calculations in the literatures.[3–5]

In H_2O/DMF/PMMA system the rate of solvent outflow (J_1) is lower than the water inflow (J_2). In this system the volume fraction of polymer decreases during the process. Figure 9 illustrates this reduction in volume fraction of polymer against the volume fraction of water in different depth of cast polymer solution (90, 140, and 240 μm). Furthermore, Figure 9 documented that all composition paths for different film thickness are the same. This result for the H_2O/DMF/PMMA system differs from the results for H_2O/AC/PMMA system. Similar results for both systems were expected in the trend but with strong differences in the quantification. However it was impossible to record a high quality spectrum for the very thin layer, thinner than 90 μm. Properly the top layer in the H_2O/DMF/PMMA system is considerably thinner than in the H_2O/AC/PMMA system reducing their influence on the polymer solution investigated.

Composition Path and Structure Formation

Composition paths can be derived from the model calculations defined in two different ways: The composition path can represent the composition range in the polymer solution between the support and the interface at a certain time. The composition path can also be defined as the composition of a certain well defined element in the solution as a function of time. On the basis of the first definition some researchers have tried to present the composition path theoretically.[3–5] The experimental data for the composition of the homogeneous polymer solution prior to precipitation of polymer are scarce; However a few attempts are recently emerged in the literatures.[6,7,31,32]

Zeman and Fraser[6] measured the variation in acetone concentration by FTIR-ATR spectroscopy during the formation of cellulose acetate membranes. For NIPS process, recently Lin and co-workers[7] have reported experimental results for the concentration variation of only water in the dope by FTIR microscopy. Fan et al.[31] and Tsai et al.[32] have used FTIR-microscopy and FTIR-ATR techniques to investigate the water penetration into polymer solution without quantifying the spectra.

In contrast to the previous works, the FTIR-ATR technique, in the present work, was used to measure directly the time dependence of components concentration (ϕ_1,ϕ_2, and ϕ_3) in the dope during the progress of NIPS process in data intervals of 0.2 sec. The ratio of solvent and water exchange in terms of $d\phi_2/d\phi_1$ was determined as presented in Figure 8 and 9. On the basis of these data the composition path is calculated and the result is shown in Figure 11 (polymer solution layer thickness was 240 μm). As stated earlier, the ratio of solvent and water exchange $d\phi_2/d\phi_1$ can

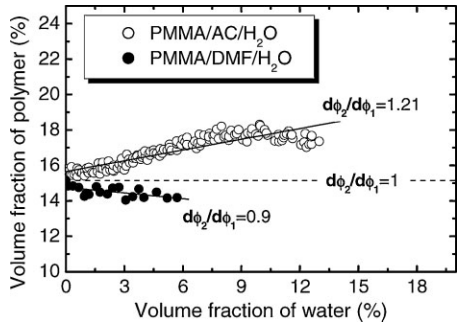

Figure 11.
Generalized relationship between volume fraction of polymer and volume fraction of water in the investigated systems.

have three distinct groups, namely, where $d\phi_2/d\phi_1 > 1, d\phi_2/d\phi_1 < 1$ and $d\phi_2/d\phi_1 = 1$. From Figure 11, in H_2O/AC/PMMA system, where $d\phi_2/d\phi_1 > 1$, the solvent release is higher than the nonsolvent penetration that leads to an increase in polymer content of the dope and the solvent moves to mix with water in the water bath. Unlike H_2O/AC/PMMA system in the H_2O/DMF/PMMA system the solvent outflow is lower than the water inflow resulting in $d\phi_2/d\phi_1 < 1$. The water penetrates into the dope to be mixed with solvent. Therefore these results show that the change of polymer concentration during the mass transfer is controlled by the relative rates of solvent release and nonsolvents penetration. Consequently the phase behavior as well as rheological properties of the system is influenced by the concentration of components in the state before phase separation.

On the other hand, the delay time in phase demixing is one of the most important parameters for analyzing the immersion precipitation process. This parameter marks the aspect of equilibrium of the process which generates so-called sponge-like structure, while instantaneous demixing connected with macrovoid formation. Kinetics is responsible for trapping specific morphologies such as macrovoidal structures. For H_2O/DMF/PMMA system, the $d\phi_2/d\phi$ is equal to 0.9, and it shows a prevailing penetration of water into the polymer solution that creates the steep gradient of chemical potential when the rapid penetration of water takes place which leads to macrovoid formation. Nonetheless, knowing the amount of flux ratio, $d\phi_2/d\phi_1$, it is necessary to analyze the structure formation. However the importance of relative rates of solvent and nonsolvent exchange can not be disclaimed. For H_2O/AC/PMMA system, the $d\phi_2/d\phi$ is equal to 1.21, and it shows a prevailing solvent release out to the polymer solution. By settling the composition path in top of the path $d\phi_2/d\phi_1 = 1$, it is observed that the structure changes to the sponge-like.

The morphology and the structures of the samples obtained in various systems are shown in Figure 12, which are formed under identical conditions. The difference in overall morphology between H_2O/AC/PMMA and H_2O/DMF/PMMA systems suggests, that the structure formation dynamics in two systems are dissimilar, as expected and observed by optical microscopy.

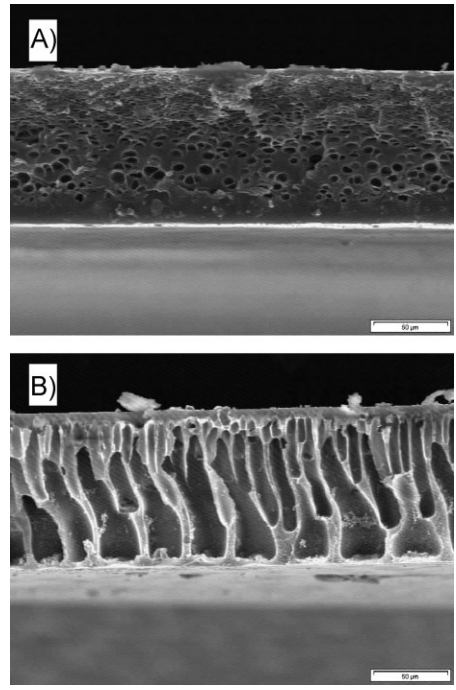

Figure 12.
SEM micrographs of PMMA membrane formed from different solvents (a - AC, b – DMF).

Conclusions

An experimental arrangement of FTIR-ATR technique and using proper computer software, was successfully adapted to measure the concentration of all components (PMMA, solvent, and water) in diffusion layers under quench condition prior to the phase separation during NISP. This technique allows a simultaneous determination of solvent outflow and water inflow through the interface. Using calibration curves the ratio of solvent and nonsolvent exchange, $d\phi_2/d\phi_1$ was determined. This term may reveal some aspects of mechanism of the structure formation.

The flux ratios, $d\phi_2/d\phi_1$ can take different values. For the H_2O/AC/PMMA system which corresponds to the delayed demixing, the water penetration was lower than the solvent release ($d\phi_2/d\phi_1 = 1.21$), whereas, for the H_2O/DMF/PMMA system which corresponds to the instantaneous demixing, the water penetration was found to be higher than solvent release ($d\phi_2/d\phi_1 = 0.9$), during the NIPS process.

The work lead to the conclusion that the FTIR-ATR is a promising tool for a better understanding of the formation of structure in membranes, it can be used for predicting the morphology and can offer possibilities for investigating the more complicated polymer solution systems. In the future it may further be used to control the structure formation.

Acknowledgements: Wolfgang Albrecht (GKSS Research Center, Teltow, Germany) and Hamid Modarress (Amirkabir University of Technology, Tehran, Iran) are thanked for their contribution in this research project.

[1] H. Strathmann, K. Kock, *Desalination* **1977**, *21*, 241.
[2] R. E. Kesting, "*Synthetic polymeric membranes*", J Wiley & Sons, New York **1985**.
[3] A. J. Reuvers, "Membrane formation: Diffusion induced demixing processes in ternary systems, PhD thesis, University of Twente", PhD thesis, The Netherlands, **1987**.
[4] C. S. Tsay, A. J. McHugh, *J. Polym. Sci., Polym. Phys. Ed.* **1987**, *28*, 1327.
[5] L. P. Cheng, Y. S. Soh, A. H. Dwan, C. C. Gryte, *J. Polym. Sci., Polym. Phys. Ed.* **1994**, *32*, 1413.
[6] L. Zeman, T. Fraser, *J. Membrane Sci.* **1994**, *87*, 267.
[7] K. Y. Lin, D. M. Wang, J. Y. Lai, *Macromolecules* **2002**, *35*, 6697.
[8] V. Gröbe, G. Mann, G. Duwe, *Faserforsch. u. Textiltechn.* **1966**, *17*, 142.
[9] R. Matz, *Desalination* **1972**, *10*, 1.
[10] M. A. Frommer, R. M. Messalem, *Ind. Eng. Chem. Prod. Res. Develop.* **1973**, *12*, 328.
[11] H. Strathmann, K. Kock, P. Amar, R. W. Baker, *Desalination* **1975**, *16*, 179.
[12] L. P. Perepechkin, V. A. Kochetova, V. P. Dubyaga, *Vysokomol. Soed. Ser. B.* **1974**, *16*, 573 (in Russian).
[13] A. J. Reuvers, J. W. A. van den Berg, C. A. Smolders, *J. Membrane Sci.* **1987**, *34*, 67.
[14] J. H. Hao, S. Wang, *J. Appl. Polymer Sci.* **2003**, *87*, 174.
[15] H. J. Kim, A. E. Fouda, K. Jonasson, *J. Appl. Polymer Sci.* **2000**, *75*, 135.
[16] F. J. Tsai, J. M. Torkelson, *Macromolecules* **1990**, *23*, 775.
[17] F. J. Tsai, J. M. Torkelson, *Macromolecules* **1990**, *23*, 4983.
[18] J. M. Cheng, D. M. Wang, F. C. Lin, J. Y. Lai, *J. Membrane Sci.* **1996**, *109*, 93.
[19] J. Y. Lin, F. C. Lin, T. T. Wu, D. M. Wang, *J. Membrane Sci.* **1999**, *155*, 31.
[20] N. J. Harrick, "*Internal Reflection Spectroscopy*", Harrick Scientific Corporation, New York **1987**.
[21] M. W. Urban, "*Attenuated Total Reflectance Spectroscopy of Polymers*", American Chemical Society, Washington, DC **1996**.
[22] TQ Analyst 6.0.0.289 Release v6, NICOLET, **1996**.
[23] I. T. Jolliffe, "*Principal component analysis*", second edition, Springer, New York **2002**.
[24] Adobe photoshop, photoshop 7.0, Release v7, **2002**.
[25] B. F. Barton, J. L. Reeve, A. J. McHugh, *J. Polymer. Sci., Polymer. Phys.* **1997**, *35*, 569.
[26] G. E. Gaides, A. J. McHugh, *J. Membrane Sic.* **1992**, *74*, 83.
[27] A. J. Mc Hugh, D. C. Miller, *J. Membrane Sci.* **1995**, *105*, 121.
[28] A. J. McHugh, C. S. Tsay, *J. Appl. Polymer Sci.* **1992**, *46*, 2011.
[29] L. Masaro, X. X. Zhu, *Prog. Polymer Sci.* **1999**, *24*, 731.
[30] G. Socrates, "*Infrared and Raman characteristic group frequencies: table and charts*", third edition, Wiley, New York **2001**.
[31] S. C. Fan, Y. C. Wang, C. L. Li, K. R. Lee, D. J. Liaw, H. P. Huang, J. Y. Lai, *J. Membrane Sci.* **2002**, *204*, 67.
[32] H. A. Tsai, M. J. Hong, G. S. Huang, Y. C. Wang, C. L. Li, K. R. Lee, J. Y. Lai, *J. Membrane Sci.* **2002**, *208*, 233.

